PIN protein phosphorylation by plant AGC3 kinases and its role in polar auxin transport

Huang, F.

Chapter 3

Redundant AGC3 kinases phosphorylate PIN auxin efflux carriers at conserved TPRXS(N/S) motifs to direct apical PIN recycling

Fang Huang*, Carlos Samuel Galván Ampudia*, Jürgen Kleine-Vehn[1], Ari Pekka Mähönen[2], Ab Quint, Ben Scheres[2], Jiří Friml[1], Remko Offringa

* These authors contributed equally to this work.

[1] Department of Plant Systems Biology, Flanders Institute for Biotechnology, 9052 Gent, Belgium.
[2] Molecular Genetics, Department of Biology, Utrecht University, 3584 CH Utrecht, The Netherlands.

Modified from Dhonukshe *et al.*, (2010) *Development*, in press

Abstract

Polar delivery of cargoes to the plasma membrane (PM) is crucial for establishing cell polarity and signaling processes. In plants, the asymmetric distribution of the PIN-FORMED (PIN) PM carriers drives polar transport of the plant hormone auxin, thereby generating the auxin maxima and minima that control plant development. The *Arabidopsis* PINOID (PID) protein kinase instructs apical PIN localization by phosphorylating PINs. Here we identify the PID homologs WAG1 and WAG2 as new PIN polarity regulators. We show that the AGC3 kinases PID, WAG1, and WAG2 and not other plant AGC kinases instruct recruitment of PINs into the apical recycling pathway by phosphorylating the middle serine residues in three conserved TPRXS(N/S) motifs within the PIN central hydrophilic loop. This phosphorylation-triggered apical PIN recycling competes with basal recycling to promote apical PIN localization. Moreover, AGC3 kinase-mediated phosphorlyation of PIN proteins enhances their PM localization, possibly by facilitating exocytosis. Our data show that by directing polar PIN localization and PIN-mediated polar auxin transport the three AGC3 kinases redundantly regulate cotyledon development, root growth and -gravitropic response, indicating their involvement in both programmed and adaptive plant development.

Introduction

Plant hormones play important roles in integrating developmental and environmental cues into signaling networks that not only shape plant architecture but also direct the plant to respond to environmental stimuli. The first identified plant hormone is auxin (indole-3-acetic acid or IAA), which directs developmental processes through its polar cell-to-cell transport-generated maxima and minima (Tanaka et al., 2006; Sorefan et al., 2009). Polar auxin transport (PAT) involves at least three types of transporter proteins, of which the PIN-FORMED (PIN) auxin efflux carriers are key drivers, as they determine the direction of auxin transport through their asymmetric subcellular localization at the plasma membrane (PM) (Wiśniewska et al., 2006).

Previously, the PINOID (PID) protein serine/threonine kinase has been identified as a positive regulator or PAT (Benjamins et al., 2001), and it controls polar targeting of PIN proteins by phosphorylating PINs in their large central hydrophylic loop (HL) (Friml et al., 2004; Michniewicz et al., 2007). Low levels of PID kinase activity (*pid* loss-of-function mutants) leads to an apical-to-basal (shootward-to rootward) switch in PIN1 polarity in the epidermis of shoot apex, resulting in pin-like inflorescences; whereas high levels of PID kinase activity (*PID* overexpression mutants) or low levels of the antagonistically acting

PP2A phosphatases (*pp2aa* phosphatase loss-of-function mutants) induce a basal-to-apical switch in PIN polarity, causing root agravitropism and primary root meristem collapse (Friml et al., 2004; Michniewicz et al., 2007). Recently, we have identified the central serine residues located in three evolutionarily conserved TPRXS(N/S) motifs in the PIN1HL as phosphorylation targets of PID, and have found that their phosphorylation is important for PIN1 function and polar targeting in *Arabidopsis* (Chapter 2; Huang et al., 2010).

The phenotypes of *pid* loss-of-function mutants (three cotyledon seedlings and pin-formed inflorescences) correlate with the tissues where *PID* is expressed, and with the changes in PIN1 polarity observed in those tissues (Benjamins et al., 2001; Friml et al., 2004). Whereas all *pid* mutants develop pin-like inflorescences as a result of the apical-to-basal PIN1 polarity alteration (Friml et al., 2004), the three cotyledon phenotype is not fully penetrant, not even in strong *pid* alleles where PIN1 localization in embryo epidermal cells is either basal or apical (Treml et al., 2005). In view of the key role of PID in PIN polar targeting, these observations strongly suggest that there are other protein kinases that act redundantly with PID in establishing PIN polarity.

PID belongs to the plant-specific ACGVIII kinase family, where it groups into the AGC3 subfamily with three other kinases (WAG1, WAG2 and AGC3-4) (Galván-Ampudia and Offringa, 2007). Here we identified the other two AGC3 kinases WAG1 and WAG2 as new determinants of PIN polarity, and showed that the central serine residue located in three conserved TPRXS(N/S) motifs in the PINHL are the key phosphorylation targets on which they act redundantly with PID, to regulate programmed embryo development and root growth in response to environmental signals, such as gravity.

Results

PID and WAG protein kinases act redundantly on PIN1 polarization during cotyledon development

To analyse whether the AGC3 kinases WAG1 and WAG2 act redundantly with PID, we used the T-DNA insertion allele *pid-14* (hereafter referred to as *pid*), and the previously characterized *wag1* and *wag2* loss-of-function mutant alleles (Santner and Watson, 2006), to generate double and triple mutant combinations.

Apart from the previously described root waving phenotype of the single and double *wag1* and *wag2* loss-of-function mutants (Santner and Watson, 2006), only *wag1* but not *wag2* showed a mild effect on embryo development (Figure 1E). Consistent with previous observations for other complete loss-of-function *pid* alleles, 47% of the *pid* mutant developed three cotyledons (Figures 1A and 1E) (Benjamins et al., 2001;

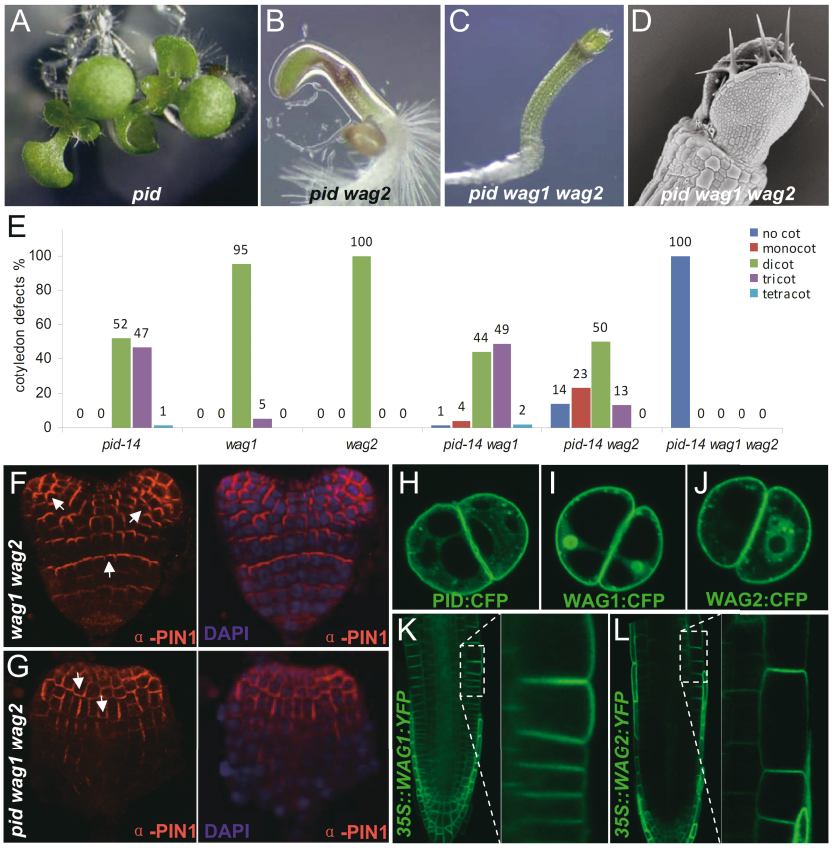

Figure 1. The AGC3 kinases PID, WAG1 and WAG2 are PM-associated proteins that act redundantly on apical PIN1 targeting during cotyledon development.

(A) to **(E)** Cotyledon phenotypes in AGC3 kinase loss-of-function mutants. **(A)** A di- and tricotyledon seedling in a *pid*+ segregating population. **(B)** A monocot *pid wag2* seedling, **(C)** A *pid wag1 wag2* seedling without cotyledons. **(D)** Scanning electron microscopy image of the apex of a no-cot *pid wag1 wag2* seedling. **(E)** Frequency of cotyledon defects observed in the indicated mutants or mutant combinations. For each mutant line, about 400 seedlings were scored for cotyledon number defects. The penetrance of the phenotypes is indicated as percentage above the bar, assuming that 1 in 4 seedlings is homozygous for the *pid* mutation.

(F) and **(G)** Whole mount immunolocalization of PIN1 in *wag1 wag2* **(F)** or *pid wag1 wag2* **(G)** mutant embryos. Left panel shows the PIN1 (Cy-3) image and the right panel shows the merge of the Cy-3 and the 4'-6-Diamidino-2-phenylindole (DAPI) image. Arrows indicate the PIN1 polarity.

(H) to **(L)** PID, WAG1 and WAG2 are PM-associated protein kinases in protoplasts **(H)** to **(J)** and in root cells **(K)** to **(L)**. The white dashed boxes in the overview image in **(K)** and **(L)** (left) indicate the position of the zoom-in image (right).

Bennett et al., 1995; Christensen et al., 2000; Friml et al., 2004). In the *pid wag1* or *pid wag2* double mutants, the penetrance of cotyledon defects remained about 50%, but a significant number of seedlings developed only one cotyledon or even lack of cotyledons

(Figures 1B-1E). This no-cotyledon phenotype was fully penetrant for the *pid wag1 wag2* triple mutant: among 99 progeny of a *pid*+ *wag1 wag2* plant, 19 were genotyped as *pid wag1 wag2* triple homozygous mutants and all lacked cotyledons (Figure 1E), whereas the remaining 80 seedlings were genotyped as *pid*+ *wag1 wag2* (n=53) or *wag1 wag2* (n=27) and developed two cotyledons. The no-cotyledon phenotype has also been observed for *pid pin1* double loss-of-function mutants (Furutani et al., 2004), suggesting that the three AGC3 kinases act redundantly on PIN1, and that this interaction is crucial for proper cotyledon development. Immunolocalization showed that PIN1 polarity was predominantly basal in epidermal cells of triple mutant embryos (Figure 1G), whereas it was apical in wild type (Friml et al., 2003b) and *wag1 wag2* mutant embryos (Figure 1F), and both apical and basal in epidermal cells of *pid* mutant embryos (Treml et al., 2005). This corroborates the redundant action of the three AGC3 kinases on apical PIN1 polarization in the embryo, which is essential for proper initiation and development of cotyledons. Our results are largely in line with the genetic data by Cheng and coworkers (Cheng et al., 2008), except that in our hands the no-cotyledon phenotype was already fully penetrant for the *pid wag1 wag2* triple mutant.

Apolar PM-associated WAG1 and WAG2 kinases induce basal-to-apical PIN polarity shifts in roots

PID is a PM-associated protein exhibiting overlapping subcellular localization with its phosphorylation targets, the PIN proteins (Michniewicz et al., 2007). Transformation of *Arabidopsis* protoplasts with the *35S::WAG1:CFP* and *35S::WAG2:CFP* constructs showed that the WAG kinases also predominantly localized at the PM (Figures 1H-1J). Complementing constructs *WAG1::WAG1:YFP* or *WAG2::WAG2:YFP* rescued *wag1 wag2* double mutant root waving phenotype, but did not lead to lines with detectable fluorescence of WAG:YFP fusion proteins (data not shown), probably due to low expression level of *WAG* genes. We therefore generated transgenic lines expressing *WAG1:YFP* and *WAG2:YFP* under control of the strong *Cauliflower Mosaic Virus 35S* promoter (*35S::WAG1:YFP* and *35S::WAG2:YFP*). In epidermis and lateral root cap (LRC) cells of seedling roots, both WAG1 and WAG2 showed a symmetric localization at the PM (Figures 1K and 1L), similar to PID.

PID overexpression has been shown to induce root agravitropism and collapse of the main root meristem (Benjamins et al., 2001). Interestingly, overexpression of *WAG1* or *WAG2* (Figures 2B and 2E, or 2C and 2F, respectively), induced root phenotypes similar to those of *PID* overexpression (Figures 2A and 2D). Immunolocalization analysis showed that PIN1, PIN2 and PIN4 were all apicalized by *PID*, *WAG1* or *WAG2* overexpression (Figures 2G to 2O), confirming our observations in *pid wag1 wag2* loss-of-function embryos and roots that the redundant activity of these kinases triggers apical

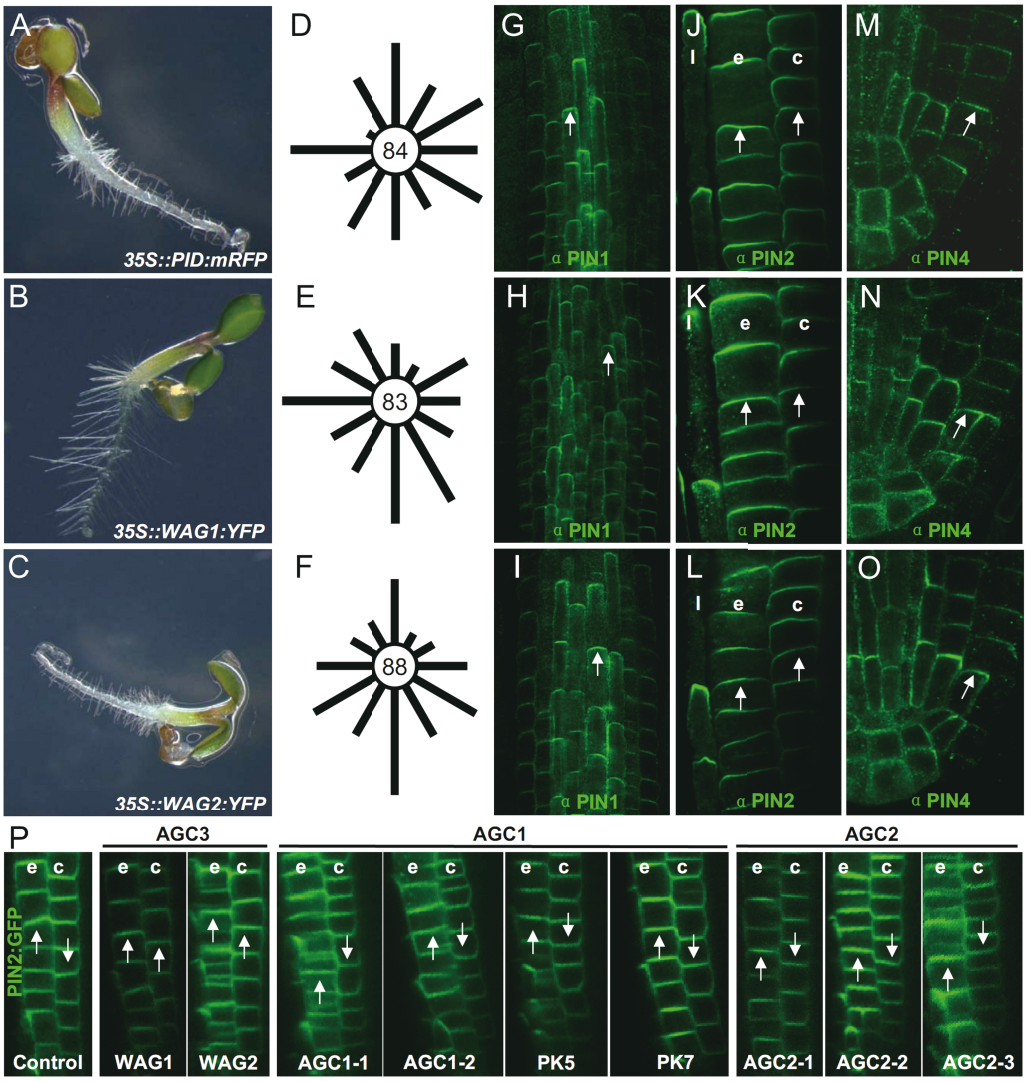

Figure 2. Overexpression of PID, WAG1 and WAG2, but not of other AGC kinases, instructs apical localization of PIN proteins, leading to agravitropic seedling growth and root meristem collapse.
(**A**) to (**O**) Overexpression of PID:mRFP **(A)**, **(D), (G), (J)** and **(M),** WAG1:YFP **(B)**, **(E), (H), (K)** and **(N)**, or WAG2:YFP **(C)**, **(F), (I), (L)** and **(O)** leads to comparable seedling phenotypes, including root meristem collapse **(A)** to **(C)**, and agravitropic root growth **(D)** to **(F)**, as a result of apical localized PIN1 in the root stele **(G)** to **(I)**, PIN2 in the cortex **(J)** to **(L)**, and PIN4 in the root meristem **(M)** to **(O)**, as shown by immunolocalization.
(P) Strong estrogen-inducible expression of WAG1 and WAG2, but not of other AGC kinases, leads to PIN2:GFP apical localization in root cortex cells. l: LRC; e: epidermis; c: cortex. White arrows indicate PIN polarity.

PIN polarization. This raised the question whether other AGC3 kinases are capable of directing PIN polarity. By using the estradiol-inducible expression system, we compared

the effect of overexpression of AGC1 (AGC1-1, also referred to as *PK64* (Mizoguchi et al., 1992) or *D6K* (Zourelidou et al., 2009), AGC1-2, PK5 and PK7) or AGC2 (AGC2-1, AGC2-2 and AGC2-3) subfamily protein kinases with that of WAG1 and WAG2 on PIN2:GFP polar localization. Only WAG1 and WAG2 induced apicalization of PIN2:GFP in root cortex cells (Figure 2P), eventually leading to root meristem collapse (data not shown), whereas the other kinases tested did not affect PIN2:GFP polarity (Figure 2P) or root meristem integrity (data not shown). These results indicate that among the AGCVIII kinases, PID, WAG1 and WAG2 are the PIN polarity regulators.

Serine residues in three conserved TPRXS(N/S) motifs in the PIN2HL are phosphorylated by AGC3 kinases *in vitro*.

Recently, we identified the central serine residue in three conserved TPRXS(N/S) motifs in the PIN1HL as phosphorylation targets of PID. Genetic and localization analysis showed that phosphorylation of these serines is important for PIN1 polar targeting and auxin-regulated embryo patterning and inflorescence development (Chapter 2; Huang et al., 2010). Comparative analysis showed that the same three motifs were present in the HL of other *Arabidopsis* PIN proteins (Huang et al., 2010), suggesting their generic importance in the regulation of the subcellular localization of the PIN family proteins.

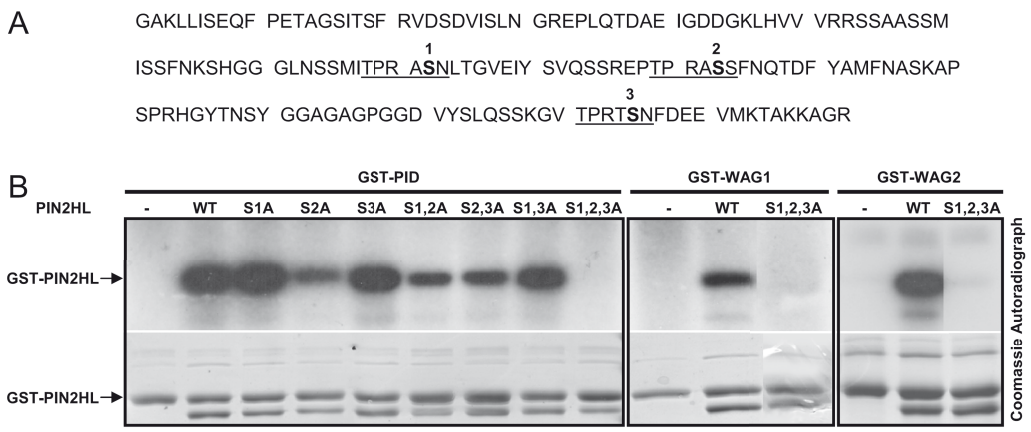

Figure 3. The central serine residue in three conserved TPRXS(N/S) motifs in the PIN2HL are the phosphorylation targets of PID, WAG1 and WAG2 kinases *in vitro*.

(A) The N-terminal sequence of the PIN2HL with the three phospho-serines in the conserved TPRXS(N/S) motifs represented by 1, 2 and 3.

(B) GST-PIN2HL is phosphorylated by GST-PID. The phosphorylation is gradually reduced when one or two serine residues are replaced with alanine (indicated as S1A, S2A, S3A, S1,2A, S2,3A, and S1,3A respectively). The phosphorylation signal is completely abolished when all three serines are mutated to alanines (S1,2,3A).

(C) GST-PIN2HL but not the GST-PIN2HL S1,2,3A mutant form is phosphorylated by GST-WAG1 and GST-WAG2.

In order to test if the three serine residues in the PIN2HL (at positions 237, 258 and 310, renumbered to 1, 2 and 3) (Figure 3A) are also PID phosphorylation targets, GST-tagged PIN2HL, or the mutant versions with the serines (S) replaced by alanines (A) were incubated with GST-PID in *in vitro* phosphorylation reactions. The results showed that all three serines were phosphorylated by PID (Figure 3B). The absence of phosphorylation signal in the GST-PIN2HL S1,2,3A mutant protein reaction indicated that the three serines are the only *in vitro* phosphorylation targets of PID in the PIN2HL. Similar results were obtained when the wild type and mutant GST-PIN2HL versions were incubated with GST-WAG1 or GST-WAG2 (Figure 3B). These results demonstrate that the three AGC3 kinases phosphorylate the PIN2HL *in vitro*, and that the substrate-specificity among the three kinases is conserved, thereby corroborating the redundant action of PID, WAG1 and WAG2 on PIN apical polarity.

Phosphorylation of conserved serines in the PIN2HL by PID, WAG1 and WAG2 controls auxin dynamics during root growth and -gravitropism

To investigate the biological significance of the AGC3 kinase-dependent phosphorylation for PIN2 *in planta*, mutations were introduced into a *PIN2::PIN2:VENUS* construct to replace all three serines (S) with alanines (A). The resulting loss-of-phosphorylation mutant construct *PIN2::PIN2:VENUS S1,2,3A*, and the wild type *PIN2::PIN2:VENUS* construct (hereafter referred to as *PIN2V SA* and *PIN2V*, respectively) were transformed into the *Arabidopsis pin2* loss-of-function allele *eir1-1*, and fluorescence positive, homozygous single locus T-DNA insertion lines were selected for further analysis.

PIN2V seedlings, germinated on 2% agar plates and placed at the 45° angle, showed root waving and gravitropic root growth (Figures 4B and 4F) similar to wild type seedlings (Figures 4A and 4F), suggesting a rescue of *eir1-1* defects by the *PIN2V* construct. In contrast, the *PIN2V SA* seedling roots exhibited a linear growth pattern interrupted by random turns, with the root tip positioned randomly towards the gravity axis (Figures 4D and 4F), similar to *eir1-1* seedling roots (Figures 4C and 4F). Consistently, *pid wag1 wag2* triple mutants also showed agravitropic root growth (Figures 4E and 4F) similar to *PIN2V SA* seedlings. In another assay, 5-days-old seedlings were reoriented 90° with the gravity vector. Wild type and *PIN2V* roots showed a normal gravitropic response (Figures 4G and 4H), whereas *eir1-1* and *PIN2V SA* mutants roots were not responsive to gravity stimulation (Figures 4I and 4J). These results proved that the *PIN2V*, but not *PIN2V SA* construct, is able to complement the root phenotypes of *pin2* mutant, and indicated that AGC3 kinase-mediated phosphorylation of PIN2 at the three conserved serines is important for PIN2-mediated root waving and gravitropic root growth.

The agravitropic root growth of the *pin2* mutant has been correlated with defective auxin distribution during gravity stimulation (Abas et al., 2006; Ottenschlager et al., 2003).

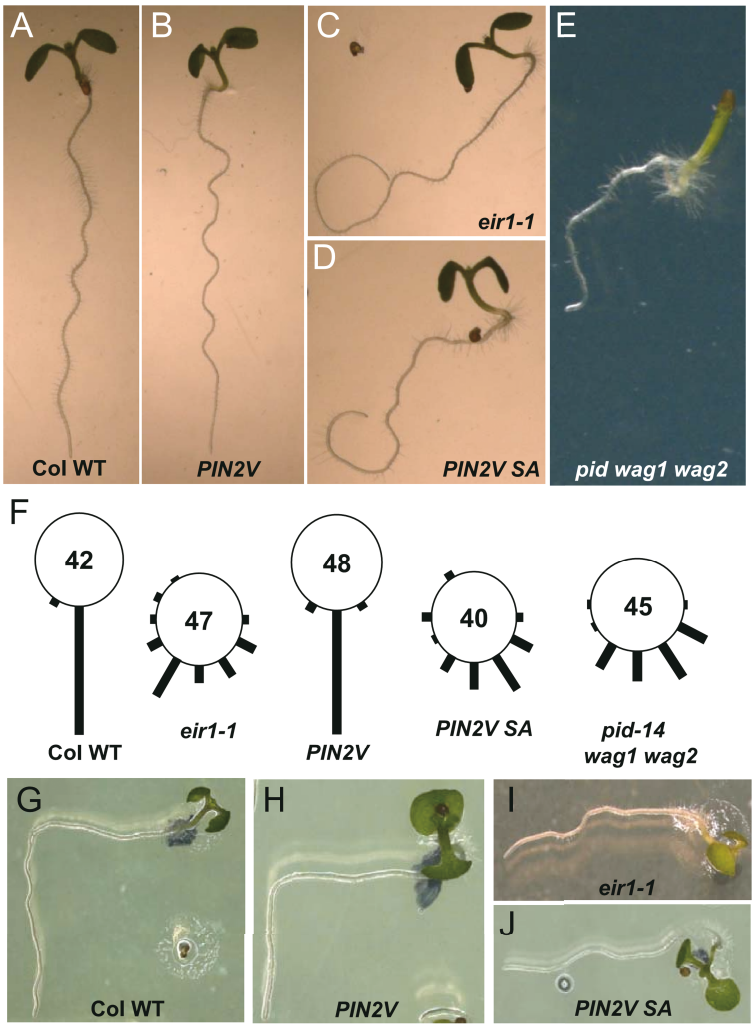

Figure 4. AGC3 kinase-phosphorylation of PIN2 is required for gravitropic root growth.
(A) to **(E)** Phenotype of 7-day-old seedling roots of Arabidopsis Columbia wild type (Col WT) **(A)**, *PIN2V* **(B)**, *eir1-1* **(C)**, *PIN2V SA* **(D)**, or *pid wag1 wag2* **(E)**
(F) Root gravitropic response histogram of the indicated lines. The number of seedlings scored per line is indicated in the middle of each circle.
(G) to **(J)** Root gravitropic analysis in Col WT **(G)**, *PIN2V* **(H)**, *eir1-1* **(I)** and *PIN2V SA* **(J)** lines

In order to know whether the observed root phenotypes in *PIN2V SA* and *pid wag1 wag2* mutants are also caused by defective auxin distribution, the mutant lines were crossed with the auxin reporter line *DR5rev::GFP* (Benková et al., 2003). The *DR5::GFP* signal was clearly enhanced in the stele and LRC in *PIN2V SA* roots compared with that in *PIN2V* roots (Figures 5A and 5B). Upon gravity stimulation, by tilting the vertically-

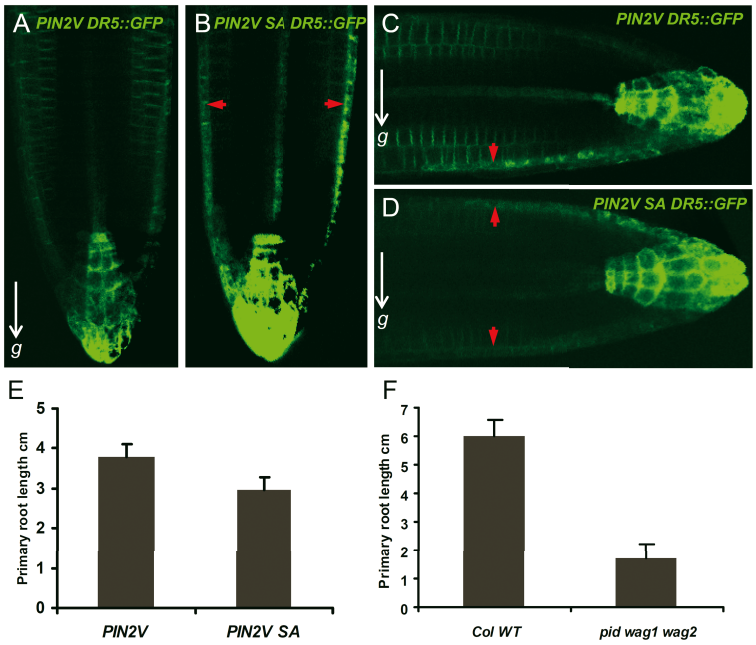

Figure 5. AGC3 kinase-phosphorylation of PIN2 is required for auxin-regulated root growth and auxin distribution.

(A) to **(D)** *DR5rev::GFP* expression in *PIN2V* **(A)** and **(C)**, or in *PIN2V SA* **(B)** and **(D)** roots grown on vertical plates **(A)** and **(B),** or extra grown for 48 hrs after tilting the vertically-grown plates 90°**(C)** and **(D)**. The white arrow indicates the gravity vector. Red arrows point out the extended GFP signal in the LRC.

(E) Ten-day-old *PIN2V SA* seedlings exhibited shorter root than that of the same age *PIN2V* seedlings.

(F) Fourteen-day-old *pid wag1 wag2* seedlings exhibited significantly shorter root than that of the same age Col WT seedlings.

growing seedlings 90°, the *DR5::GFP* signal in *PIN2V SA* roots remained symmetrically distributed to both sides of the LRC (Figure 5D). A similar distribution was observed in *pid wag1 wag2* mutant roots (data not shown). In contrast, *PIN2V* roots showed an enhanced *DR5::GFP* signal at the lower side of the root tip (Figure 5C), consistent with previous reports (Abas et al., 2006). Further analysis of root length showed that both *PIN2V SA* and *pid wag1 wag2* mutants developed significantly shorter roots (Figures 5E and 5F), most likely caused by the higher auxin accumulation in the root tip (Figures 5A and 5B).

AGC3 kinases control apical PIN2 polarity in young epidermal cells of the root tip

To correlate the phenotypes and changes in auxin dynamics in the *PIN2V SA* and *pid wag1 wag2* mutant roots with changes in PIN2 polarity, we observed *PIN2V SA* directly by confocal microscopy or following whole mount immunolocalization using PIN2-specific

antibodies. In agreement with previous observations for PIN2 or PIN2:GFP (Müller et al., 1998; Abas et al., 2006), PIN2V was apically localized in LRC and epidermal cells, and showed basal localization in young cortical cells (Figure 6A and zoom-in image), and a basal-to-apical shift in older cortical cells. In contrast, PIN2V SA was basally localized in young epidermis and cortex cells of the distal root tip, whereas older epidermis and cortex cells showed a gradual basal-to-apical shift (Figure 6B and zoom-in image). A similar PIN2 localization pattern was observed in *pid wag1 wag2* triple mutant roots (Figure 6D), but not in *pid+ wag1 wag2* roots (Figure 6C), suggesting that a single copy of the *PID* gene is sufficient to restore PIN2 wild type localization. These results corroborated that the changes of auxin distribution observed in *PIN2V SA* and *pid wag1 wag2* mutants are due to disturbed polar localization of PIN2, as a result of loss of phosphorylation.

PID overexpression induces a basal-to-apical PIN2 polarity shift in cortical cells of

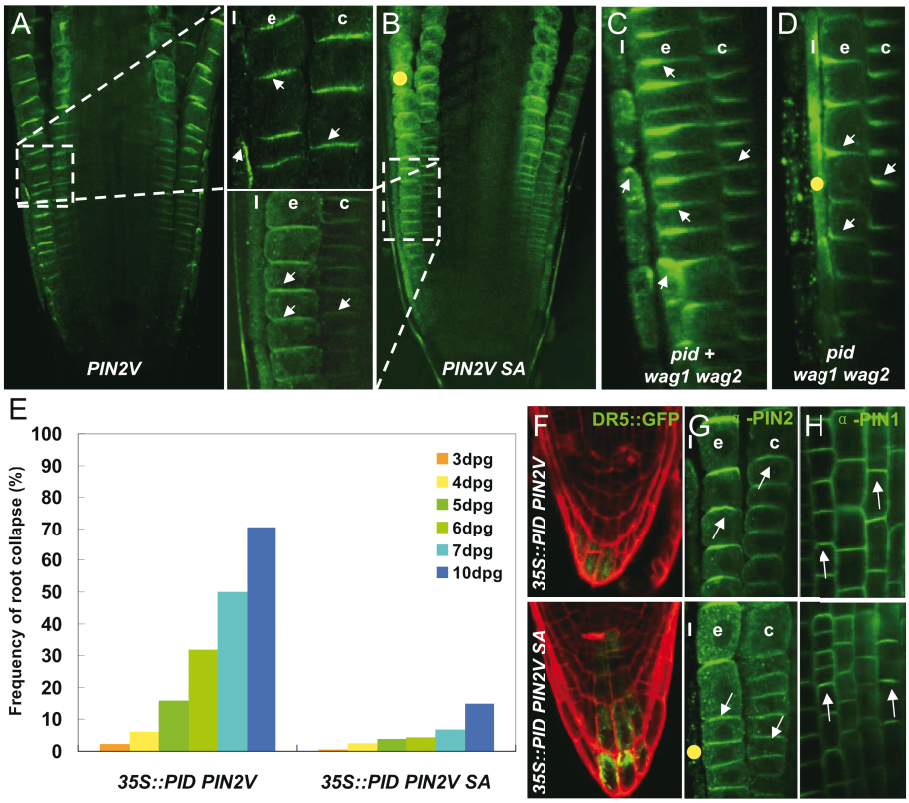

Figure 6. AGC3 kinase-mediated phosphorylation of the conserved serines is required for proper apical PIN2 localization in root epidermis and LRC cells**.**

(A) to **(D)** Whole mount immunolocalization of PIN2 in 5-day-old seedling roots of the *PIN2V* **(A)** and *PIN2V SA* **(B)** lines, or the *pid+ wag1 wag2* **(C)** and *pid wag1 wag2* triple mutants **(D)**. *pid+* indicates that the seedling

the root, and results in depletion of the auxin maximum in root tips (Friml et al., 2004). Expression of the PIN2V SA protein in the *35S::PID* background significantly delayed *PID* overexpression-induced root collapse (Figure 6E), correlating with a stronger *DR5::GFP* signal in the collumella (Figure 6F). Whereas *PID* overexpression induced PIN2V apicalization, PIN2V SA localization in both epidermal and cortical cells was not responsive to *PID* overexpression and exhibited the same polarity as that in the wild type background (Figure 6G). In the same roots of the *PIN2V* and *PIN2V SA* mutant lines, *PID* overexpression induced PIN1 targeting to the apical side (Figure 6H), demonstrating that *PID* overexpression in these seedlings was sufficient to induce a basal-to-apical shift of PIN polarity, and that the PIN2V SA protein is insensitive to PID activity due to the absence of PID phosphorylation targets.

These results are in line with the above observations on the redundant role of the three AGC3 kinases in instructing apical localization of PIN proteins by phosphorylating the three TPRXS(N/S) motifs, but also indicate that in specific cell types, such as older epidermal and cortex cells, PIN apicalization probably involves an AGC3-unrelated regulatory mechanism.

PIN2 loss-of-phosphorylation enhances its endosomal accumulation and induces recruitment into the basal recycling pathway

Notably, the PIN2V SA PM signal in LRC cells was lost, and an enhanced intracellular signal was detected in LRC and in root epidermis and cortex cells (Figure 6B), as compared to PIN2V (Figure 6A). This enhanced internal localization was also observed for PIN2 in the same cell files in the *pid wag1 wag2* mutant (Figure 6D). In order to characterize these internal signals, seedlings were incubated for 10 minutes with the endocytotic tracer FM4-64. The internalized PIN2V SA signal was found to colocalize with FM4-64 stained endosomes (Figure 7A), suggesting that PIN2V SA was internalized to the endosomes.

It is known that PIN proteins undergo constitutive recycling between PM and endosomes, and that GNOM-dependent basal recycling is sensitive to the fungal toxin

is heterozygous for the *pid* loss-of-function mutation. The white dashed boxes in the overview images **(A)** and **(B)** indicate the position of the zoom-in images. Internalized PIN2 signal in the LRC cells is marked with yellow dots. PIN polarity is indicated with white arrows. l: LRC; e: epidermis; c: cortex.

(E) and **(F)** The root meristem collapse induced by *PID* overexpression is partly rescued by *PIN2V SA* **(E)**, due to a higher *DR5rev:GFP* signal in *35S::PID PIN2V SA* than that in *35S::PID PIN2V* **(F)**.The frequency was determined by monitoring the onset of root meristem collapse in 132, 162 seedlings, respectively.

(G) and **(H)** Immunolocalization of PIN2 **(G)** and PIN1 **(H)** in 3-day-old *35S::PID PIN2V* or *35S::PID PIN2V SA* seedling roots. White arrows indicate PIN polarity, and the yellow dot marks the internalized PIN2 signals in LRC cells.

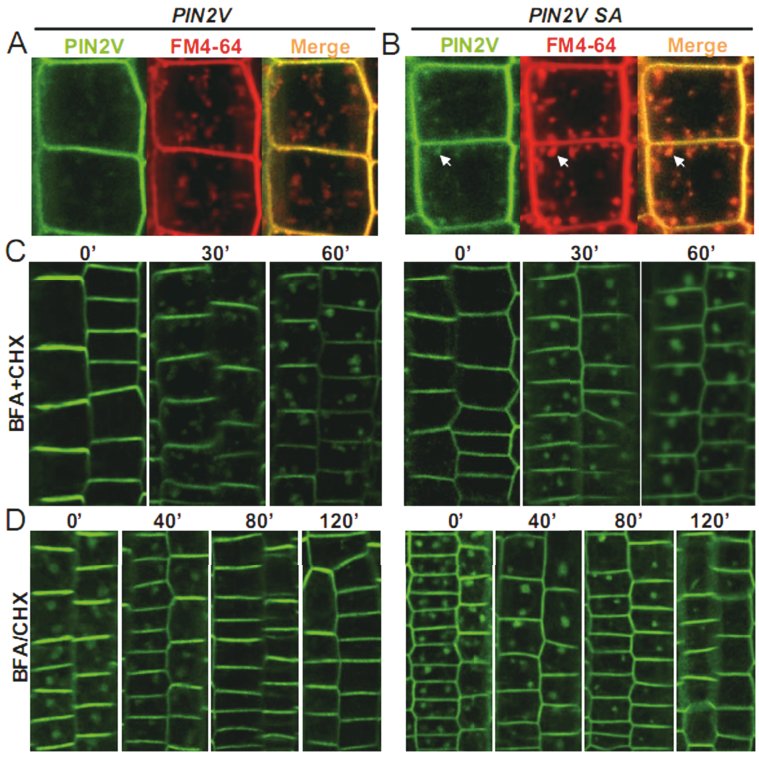

Figure 7. PIN2 loss-of-phosphorylation results in enhanced endosomal localization and its recruitment in the basal recycling pathway.

(A) and **(B)** Co-localization of internalized PIN2V **(A)** or PIN2V SA **(B)** in root epidermal cells of 5-day-old seedlings with the endocytic tracer FM4-64.

(C) Time lapse of intracellular accumulation of PIN2V or PIN2V SA in root epidermal cells of 5-day-old seedlings treated with 50 μM BFA, in the presence of 50 μM of the protein synthesis inibitor cycloheximide (CHX)

(D) Time lapse of the effect of BFA washout in the presence of 50 μM CHX on PIN2V or PIN2V SA intracellular accumulation in root epidermal cells of 5-day-old seedlings.

brefeldin A (BFA), whereas apical recycling pathway is mediated by a BFA resistant ARF-GEF (Geldner et al., 2001; Kleine-Vehn et al., 2008a). In order to further demonstrate the differential localization of the PIN2V and PIN2V SA proteins in young epidermal cells in the root tip, *PIN2V* and *PIN2V SA* seedlings were treated with BFA, and time-lapse imaging showed that PIN2V SA accumulated more rapidly in BFA compartments than PIN2V (Figure 7C). This indicated that loss-of-phosphorylation mutant PIN2V SA protein is predominantly localized in the basal recycling pathway, whereas PIN2V localized to the opposite BFA resistant pathway. When BFA was washed out, the BFA-induced intracellular accumulation for both PIN2V and PIN2V SA was fully reversible but with different rates (Figure 7D), demonstrating that both endocytosis and exocytosis steps

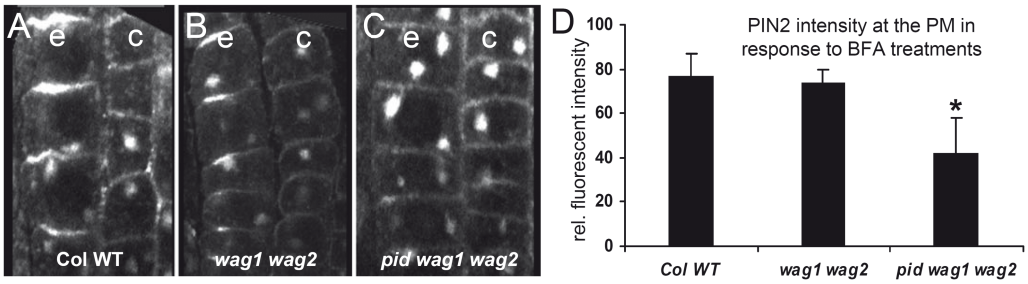

Figure 8. Loss of AGC3 kinases activity induces stronger sensitivity of PIN2 to BFA treatment.
(A) to **(C)** BFA treatment induces stronger PIN2 accumulation in the BFA compartment in *pid wag1 wag2* mutant **(C),** than in Col WT **(A)** or *wag1 wag2* double mutant **(B)**.
(D) The PIN2 intensity at the PM in response to BFA treatments is significantly reduced in *pid wag1 wag2* triple mutant roots. The PIN2 intensity at the PM in young epidermal cells of Columbia wild type (Col WT), *wag1 wag2* or *pid wag1 wag2* roots was measured with Image j. n=30 cells; Asterisk above the error bar indicates significantly different with WT in the Student's t-test (p=0,0001).

are functional, and that the differential effects of BFA on PIN2V and PIN2V SA is the result of their distinct polarity. The re-establishment of PM localization after BFA removal was independent of *de novo* protein biosynthesis, as the experiments were performed in the presence of the protein synthesis inhibitor cycloheximide (CHX). In line with these observations, PIN2 accumulation into BFA compartments in root epidermal cells was enhanced in *pid wag1 wag2* mutant roots (Figure 8C) compared to wild type (Figure 8A) or *wag1 wag2* double mutant roots (Figure 8B), as PIN2 apicalization in the epidermal cells was significantly reduced (Figure 8D).

Our data show that non-phosphorylated PIN2 is recruited into the basal recycling pathway, and that at the same time loss-of-phosphorylation reduces PIN PM localization and results in enhanced endosomal localization. The latter observation is in line with the proposed role for PID and the redundantly acting WAG kinases as positive regulators of auxin efflux.

Discussion

PID and its closely related protein kinases WAG1 and WAG2 function redundantly in both programmed and adaptive plant development.

The AGC3 kinases have been shown to function redundantly in embryo development, as simultaneous disruption of the four genes encoding these kinases completely abolished cotyledon formation (Cheng et al., 2008). Our analysis showed, however, that disruption of three genes (*PID, WAG1* and *WAG2*) is already sufficient to abolish cotyledon formation, suggesting that the fourth gene *AGC3-4*/*PID2* may not be essential

for cotyledon initiation. This conclusion is supported by the expression of the *AGC3* genes, showing that *PID2* is expressed in the provascular cells of the embryo, whereas *PID, WAG1* and *WAG2* are expressed in the empidermis of young embryos (Cheng et al., 2008), where they are required to instruct apical PIN1 localization.

Based on the phenotypes of the *pid* loss-of-function mutant in the embryo and inflorescence, the PID kinase has initially been considered as regulator of programmed plant development (Christensen et al., 2000; Benjamins et al., 2001). The strong wavy root phenotype of the *wag1 wag2* double mutant (Santner and Watson, 2006), the mild agravitropic roots of *pid* mutant (Sukumar et al., 2009), and our observations that both the *pid wag1 wag2* and the *PIN2V SA* loss-of-phosphorylation mutant roots are strongly affected in root waving and gravitropic growth, now point to a novel role for these three kinases in adaptive plant development. The impairment of apical PIN2 polarity in the absence of PID, WAG1 and WAG2 leads to altered auxin distribution, resulting in a reduced root length and agravitropic root growth.

The AGC3 kinases PID, WAG1 and WAG2 direct PIN polarity through a conserved mechanism.

Previously, we have shown that the PID kinase and PP2A phosphatases act antagonistically on PIN polarization by determining the phosphorylation status of the PINHL (Friml et al., 2004; Michniewicz et al., 2007). Here we identified two PID-related kinases, WAG1 and WAG2, as novel PIN polarity determinants similar to PID. Our analysis is seemingly contradictory to the observed inverse regulation of *PID* and *WAG2* expression during valve margin specification in fruits that correlated with PIN3 polarity changes (Sorefan et al., 2009). However, the effect of the kinases on PIN polarity might depend on tissue specific factors, which may be different in embryos or seedlings than in fruits.

PID and the WAG kinases belong to the plant specific AGCVIII family of kinases, where they cluster into the AGC3 subfamily (Galván and Offringa, 2007). Inducible expression of different AGCVIII kinases showed that only PID, WAG1 and WAG2 but not other AGC kinases can trigger a basal-to-apical shift in PIN2 polarity, suggesting that the regulation of PIN polarity is specific for AGC3 kinases. This AGC3 kinase-regulated PIN polar localization is determined by the phosphorylation of PIN2HL at the same three serine residues, which are conserved in all *Arabidopsis* PM PIN proteins (Chapter 2; Huang et al., 2010), providing the evidence that PID, WAG1 and WAG2 regulate PIN polarity through a conserved mechanisms. Recently, it has been shown that the D6 kinases (AGC1-1, AGC1-2, PK6 and PK5), which are involved in PAT, also phosphorylate the PIN1HL, but do not affect PIN polarity (Zourelidou et al., 2009). Although the phosphorylation sites of the D6 kinases are still unknown, it is likely that they

have different targets in the PIN1HL from our identified TPRXS(N/S) motifs. Alternatively, they may only phosphorylate one or two of our identified serines, which will not lead to a polarity switch, as simultaneous phosphorylation of the three serines is necessary for proper apical PIN targeting (Chapter 2; Huang et al., 2010). Detailed analysis of the phosphorylation specificity of the D6 kinases will provide further insight into this issue.

AGC3 kinase mediated phosphorylation instructs PIN recruitment into the apical recycling pathway and enhances PIN PM localization

Apically-localized PIN proteins are less sensitive to BFA treatment than basally-localized PINs (Geldner et al., 2003; Kleine-Vehn et al., 2008a). Accordingly, it has recently been shown that PID-dependent phosphorylation of PIN1 is required for its recruitment from basal to the apical recycling pathway (Kleine-Vehn et al., 2009). Here, we showed that loss-of-phosphorylation PIN2V SA is more sensitive to BFA than wild type PIN2V, and exhibits apical-to-basal polarity alteration in the young epidermal cells of the root tip, confirming that PIN phosphorylation by these three kinases reduces their affinity for the basal, BFA-sensitive recycling pathway, and instructs their recruitment in the apical BFA-insensitive recycling pathway.

Interestingly, however, in the *pid wag1 wag2* triple mutant or in the *PIN2V SA* line, the PIN2 apical-to-basal polarity switch in epidermis cells is not complete, as in older epidermis cells in de elongation/differentiation zone of the root, PIN2 is still predominantly localized at the apical side, indicating that in some cell files PIN apicalization probably involves an AGC3 kinase-unrelated mechanism. Besides predominantly apical PIN2 localization, strong internalized PIN2 signals were detected in these older root epidermis and LRC cells in *PIN2V SA* and *pid wag1 wag2* mutants. Similar internalization of PINs has been observed for loss-of-phosphorylation PIN1:GFP proteins in the embryo (Chapter 2; Huang et al., 2010), and for PIN2 in the *pid* mutant root (Sukumar et al., 2009). Together, these results suggest that phosphorylation by the three AGC3 kinases is important for the maintenance of PIN proteins at the PM. Based on the enhanced recovery of PIN2V PM abundance, as compared to PIN2V SA in the BFA wash out experiments, it is likely that phosphorylation promotes exocytosis, and that non-phosphorylated PINs show enhanced internalization due to reduced exocytosis. Further genetic and cellular analysis should help to firmly establish which trafficking pathway is influenced by phosphorylation.

In conclusion, our findings indicate that the three AGC3 kinases act redundantly in programmed plant development as well as in developmental plasticity in response to environmental stimuli, and that they orient plant development by instructing the subcellular distribution of PIN auxin efflux carriers by phosphorylation of the conserved serine residues in the PINHL. In combination with our data showing the importance of

the phosphorylation status of the TPRXS(N/S) motifs in PIN1 (Chapter 2; Huang et al., 2010), these results provide further evidence for our hypothesis that phosphorylation of the consensus serines by AGC3 kinases arose as a conserved mechanism to regulate the subcellular localization and function of PIN family proteins throughout the evolution of land plants (Galván-Ampudia and Offringa, 2007).

Materials and methods

Plant lines, growth conditions and plant transformation

For all experiments, *Arabidopsis thaliana* Columbia-0 (Col-0) ecotype was used. The mutants *pid-14* (SALK_049736), *wag1* (SALK_002056), *wag2* (SALK_070240) and *eir1-1* were described before (Bennett et al., 1995; Luschnig et al., 1998; Santner and Watson, 2006). For the T-DNA insertion mutants *pid-14*, *wag1* and *wag2*, the following gene-specific primers (Table 1) were used to detect T-DNA insertion: PIDex1 F1 - PIDex2 R1 for *pid-14*, N502056 F - N502056 R for *wag1*, and N570240 F - N570240 R for *wag2*. T-DNA specific primers were LB1a for the SALK lines and LB2 for the SAIL line.

Seeds were surface sterilized with 50% commercial bleach solution for 10 minutes and rinsed with sterile water. Seeds were germinated on MA medium (Masson and Paszkowski, 1992) supplemented with antibiotics when required and vernalized 3 days at 4ºC in darkness. Seedlings were grown in a 16 hrs light/ 8 hrs dark cycle at 21ºC. Two-week-old plants were transferred to soil and grown in growth room at 21ºC, 16 h photoperiod and 70% relative humidity.

Arabidopsis thaliana Col-0 wild type (Col WT) or the *eir1-1* mutant plants were transformed by the floral dip method as described (Clough and Bent, 1998) using *Agrobacterium* strain AGL1 (Lazo et al., 1991). Primary transformants were selected on medium supplemented with 100 µg/ml timentin and 30 µg/ml nystatin to inhibit *Agrobacterium* growth, and with 100 µg/ml gentamicin (Gm), 20 µg/ml hygromycin (Hm) or 30 µg/ml phosphinothricin (PPT) for constructs *pPZP221-PIN2::PIN2:VENUS*, *pGreenII0179*, or *pGreenII0229*, respectively.

Molecular cloning, DNA constructs and mutagenesis

Molecular cloning was performed following standard procedures (Sambrook et al., 1989). The coding region of *PID* was amplified from *Arabidopsis thaliana* ecotype Columbia (Col-0) cDNA from siliques using primer set PID attB F and PID -Stop attB R (Table 1). Coding regions for *WAG* genes were PCR amplified from *Arabidopsis thaliana* Col-0 genomic DNA using respectively primer sets WAG1 attB F - WAG1 –Stop attB R, and WAG2 attB F - WAG2 –Stop attB R (Table 1). Expression vectors *pGEX-WAG1*, *pGEX-WAG2*,

Table 1. Primer list for DNA recombination and genotyping

Primer names	Sequence (5' to 3')
PID attB F	GGGGACAAGTTTGTACAAAAAAGCAGGCTTCAGCATGTTACGAGAATCAGACGGT
PID –Stop attB R	GGGGACCACTTTGTACAAGAAAGCTGGGTCAAAGTAATCGAACGCCGCTGG
WAG1 attB F	GGGGACAAGTTTGTACAAAAAAGCAGGCTTCAGCATGGAAGACGACGGTTATTAC
WAG1 –Stop attB R	GGGGACCACTTTGTACAAGAAAGCTGGGTCTAGCTTTTTACCCACATAATG
WAG2 attB F	GGGGACAAGTTTGTACAAAAAAGCAGGCTTCAGCATGGAACAAGAAGATTTCTAT
WAG2 –Stop attB R	GGGGACCACTTTGTACAAGAAAGCTGGGTCAACGCGTTTGCGACTCGCGTA
PIDex1 F1	TCTCTTCCGCCAGGTAAAAA
PIDex2 R1	CGCAAGACTCGTTGGAAAAG
N502056 F	TCTCGCACGCTCAAGCCTAAC
N502056 R	CACCAATCTACACCGCTTCCG
N570240 F	TCTTCTACGACGAAGCGACGG
N570240 R	CTATCAAGTCTCCAATGTCTTCTTT
LB1a	TGGTTCACGTAGTGGGCCATCG
LB2	GCTTCCTATTATATCTTCCCAAATTACCAATACA
agc1-1F-attB1	GGGGACAAGTTTGTACAAAAAAGCAGGCTAAACAATGATGGCTTCAAAAACTCCAGAAGG
agc1-1R-attB2	GGGGACCACTTTGTACAAGAAAGCTGGGTGTCAGAAGAAATCAAACTCAAGATAATTACTCTGATCA
agc1-2F-attB1	GGGGACAAGTTTGTACAAAAAAGCAGGCTAAACAATGGCCTCGAAGTATGGTTCTGG
agc1-2R-attB2	GGGGACCACTTTGTACAAGAAAGCTGGGTGTCAAAAGAAATCGAACTCCAGATAATTACTCTGGTC
agc2-1F-attB1	GGGGACAAGTTTGTACAAAAAAGCAGGCTAAACAATGCTAGAGGGAGATGAGAAACAG
agc2-1R-attB2	GGGGACCACTTTGTACAAGAAAGCTGGGTGTTAAAATACCAAAAAATTGTTATCACTTTCTAAATCGTG
agc2-3F-attB1	GGGGACAAGTTTGTACAAAAAAGCAGGCTAAACAATGGAGACAAGACCATCATCATCATCTTCTCTTTC
agc2-3R-attB2	GGGGACCACTTTGTACAAGAAAGCTGGGTGTCAGAAATCAACAAACGGATTGTTTTCAGAACACTC
agc2-4F-attB1	GGGGACAAGTTTGTACAAAAAAGCAGGCTAAACAATGGAGCCATCACCGTCGTC
agc2-4R-attB2	GGGGACCACTTTGTACAAGAAAGCTGGGTGTTAGAATTCAATAAACGGATCGTTTTTACGACACAC
wag1F-attB1	GGGGACAAGTTTGTACAAAAAAGCAGGCTAAACAATGGAAGACGACGGTTATTACCTCG
wag1R-attB2	GGGGACCACTTTGTACAAGAAAGCTGGGTGTTATAGCTTTTTACCCACATAATGATAGTAATTATTATTGCTCTG
wag2F-attB1	GGGGACAAGTTTGTACAAAAAAGCAGGCTAAACAATGGAACAAGAAGATTTCTATTTCCCTGACACCGA
wag2R-attB2	GGGGACCACTTTGTACAAGAAAGCTGGGTGTTAAACGCGTTTGCGACTCGCGT
AtPK5F-attB1	GGGGACAAGTTTGTACAAAAAAGCAGGCTAAACAATGGCGTCCACTCGTAAACC
AtPK5R-attB2	GGGGACCACTTTGTACAAGAAAGCTGGGTGCTAGAAGAAATCAAATTCCAAATAGTTATCAGACCCT
AtPK7F-attB1	GGGGACAAGTTTGTACAAAAAAGCAGGCTAAACAATGGATTCTTCTTCATCAGTCGTTTACGTTGG
AtPK7R-attB2	GGGGACCACTTTGTACAAGAAAGCTGGGTGTCAGAAGAAATCAATTTCCAAATAATTACCAGAAGGCT

pART7-PID:CFP, *pART7-PID:mRFP*, *pART7-WAG1:YFP*, *pART7-WAG1:CFP*, *pART7-WAG2:YFP*, *pART7-WAG2:CFP*, *pGreenII0179-WAG1::WAG1:YFP* and *pGreenII0179-WAG2::WAG2:YFP* were constructed using the Gateway technology (Invitrogen). Overexpression cassettes containing the genes of interest were digested with *Not I* and cloned into *pGreenII* binary vectors for *Agrobacterium*-mediated transformation of *Arabidopsis thaliana*. The *pPZP221-PIN2::PIN2:VENUS* construct was kindly provided by Christian Luschnig.

Table 2. Primer list for mutagenesis

Primer names	Sequence (5' to 3')
PIN2HL S237A F	CATGATAACGCCGCGAGCTGCAAATCTCACC
PIN2HL S237A R	GGTGAGATTTGCAGCTCGCGGCGTTATCATG
PIN2HL S258A F	CCGACGCCGAGAGCTGCTAGCTTTAATCAG
PIN2HL S258A R	CTGATTAAAGCTAGCAGCTCTCGGCGTCGG
PIN2HL S310A F	CGTGACGCCGAGAACGGCAAATTTTGATGAGG
PIN2HL S310A R	CCTCATCAAAATTTGCCGTTCTCGGCGTCACG
PIN2HL S237E F	CATGATAACGCCGCGAGCTGAAAATCTCACCGG
PIN2HL S237E R	CCGGTGAGATTTTCAGCTCGCGGCGTTATCATG
PIN2HL S258E F	GCCGACGCCGAGAGCTGAGAGCTTTAATCAG
PIN2HL S258E R	CTGATTAAAGCTCTCAGCTCTCGGCGTCGGC
PIN2HL S310E F	GGCGTGACGCCGAGAACGGAAAATTTTGATGAGG
PIN2HL S310E R	CCTCATCAAAATTTTCCGTTCTCGGCGTCACGCC

For *pART7*-based destination vectors the recombination cassette was inserted in frame with the *YFP*, *CFP* or *mRFP1* coding region between the *CaMV 35S* promoter and, the *CaMV 35S* terminator. For the *pGEX*-based destination vector, the recombination cassette was inserted in frame with the *GST* coding region. For the *pGreenII*-based destination vector, the recombination cassette was inserted in frame with the *YFP* coding region and the *CaMV 35S* terminator into *pGreenII0179* (Galván-Ampudia and Robert, unpublished data). Bacteria were grown on LC medium supplemented with 100 µg/mLcarbenicillin (Cb) or 10 µg/mL gentamicin for *E. coli* strain DH5α containing *pDONR207*, *pART7* or *pGEX*-based plasmids, or 50 µg/mL kanamycin (Km) for *E. coli* strain DH5α or *Agrobacterium tumefaciens* strain AGL1 (Lazo et al., 1991) containing *pGreenII*-based binary vectors (Hellens et al., 2000). For AGL1 20 µg/ml rifampicin was included in the LC medium.

The constructs *pGEX-PID* (Benjamins et al., 2003) and *pGEX-PIN2HL* (Abas et al., 2006) have been described before. The Quickchange XL site-directed mutagenesis kit (Stratagene) was used to generate mutant constructs. Oligonucleotides used for mutagenesis are listed in Table 2.

For the AGC kinase inducible overexpression studies, a modified version of pER8 was used (Zuo et al., 2000). Strong and ubiquitously expressed 243 bp pG10-90 promoter (Zuo et al., 2000) was cloned into the promoter box and the AGC kinase genes were amplified from Col WT genomic DNA (for primers see Table 1) and cloned into the gene box of the Multisite gateway vectors (Invitrogen). Modified pER8 vector was

cloned into the first box of the Multisite gateway to allow easy cloning of genes (2nd box) and terminators or reporter fusions (3rd box). Details of the inducible system will be described elsewhere (Mähönen, A.P. and Scheres, B., manuscript in preparation).

Protein purification and *in vitro* phosphorylation assays

GST-tagged PID, WAG1 and WAG2 and wild type or mutant PIN2HL proteins were purified and used in *in vitro* phosphorylation assays. Cultures of *E. coli* strain Rosetta (Novagen) containing the constructs were grown at 37ºC to OD_{600}=0.6 in LC supplemented with 100 µg/mL carbenicillin (Cb) and 34 µg/mL chloramphenicol. The cultures were then induced for 4 hrs with 1 mM IPTG at 30ºC, harvested by centrifugation and frozen at -20ºC. Pelleted cells were resuspended in extraction buffer (EB: 1x PBS, 2 mM EDTA, 2 mM DTT) supplemented with 0.1% Tween-20 and 0.1 mM of the protease inhibitors Phenylmethanesulfonyl fluoride, leupeptin and aprotinin (Sigma) and sonicated. Sonicates were centrifugated at 14,000 RPM for 20 min, and supernatants were incubated 1 hr with 100 µL Glutathione Sepharose (GE Amersham) and subsequently washed 3 times with EB. Purified proteins were recover with glutathione elution buffer (reduced glutathione 10 mM, Tris-HCl pH 8.0 50 mM), diluted 1000-fold in Tris buffer (25 mM Tris-HCl pH 7.5; 1 mM DTT) and concentrated using Vivaspin microconcentrators (Vivascience).

Approximately 1 µg of each purified GST-tag proteins (kinase and substrates) were added to a 20 µl kinase reaction mix, containing 1x kinase buffer (25 mM Tris-HCl pH 7.5, 1 mM DTT, 5 mM $MgCl_2$) and 1x ATP solution (100 µM $MgCl_2$, 100 µM ATP-Na^{2+}, 1 µCi ^{32}P-γ-ATP), incubated at 30ºC for 30 minutes and stopped by addition of 5 µL of 5x protein loading buffer (310 mM Tris-HCl pH 6.8, 10% SDS, 50% Glycerol, 750 mM β-Mercaptoethanol, 0.125% Bromophenol Blue). Reactions were subsequently separated over 10% acrylamide gels, which were washed three times for 30 minutes with kinase gel wash buffer (5% Trichloroacetic Acid, 1% $Na_2H_2P_2O_7$), Coomassie stained and dried. Autoradiography was performed for 24-48 hrs at -80ºC using Fuji Super RX X-ray films and intensifier screens.

Protoplast isolation and transformation

Arabidopsis thaliana Col-0 cell suspension cultures were used for protoplast preparations. Culture maintenance, protoplast isolation and transfections were performed as previously described (Schirawski et al., 2000) with minor modifications. Four-to-six days old cultures were diluted 5-fold in auxin-free Cell Medium (30 g/L saccharose, 3.2 g/L Gamborg's B5 basal medium with mineral organics, adjusted to pH 5.8 with KOH and sterilized by autoclaving), incubated overnight and used for protoplast isolation in auxin-free solutions. Transfected cells were kept at 25ºC in the dark for 16-18 hrs before

treatments.

Drug application and experimental conditions

Exogenous drugs were applied by incubating 5-day-old seedlings in liquid MA medium supplemented with BFA (50 mM stock in dimethylsulfoxide [DMSO]) (50 μM), cycloheximide (50 mM stock in DMSO) (50 μM). Control treatments contained an equivalent amount of solvent (DMSO). For BFA washout experiments (concomitant cycloheximide and BFA pretreatment for 1 hr), seedlings were rinsed three times in liquid MA medium (conditionally supplemented with cycloheximide) and subsequently washed in MA medium (conditionally supplemented with cycloheximide) for the indicated time periods.

Immunolocalization and confocal microscopy

Whole-mount immunolocalizations were performed on 3-5 days old seedlings fixed in 4% paraformaldehyde in MTSB buffer as described previously (Friml et al., 2003a) with an InSituPro robot (INTAVIS, Cologne, Germany). Rabbit anti-PIN1 (Friml et al., 2004), anti-PIN2(Abas et al., 2006) and anti PIN4 (Friml et al., 2002a) primary antibodies (1/200) and Alexa (1/200, Molecular Probes) conjugated anti-rabbit secondary antibodies were used for detection.

Samples were observed using confocal laser scanning microscopy. GFP fusion lines and immunolocalization signals were observed using 40x dry objectives on a ZEISS Axioplan microscope equipped with a confocal laser scanning unit (MRC1024ES, BIO-RAD, Hercules, CA). The GFP fluorescence was monitored with a 522-532 nm band pass emission filter (488 nm excitation). All images were recorded using a 3CCD Sony DKC5000 digital camera. For the protoplast experiments, a Leica DM IRBE confocal laser scanning microscope was used with a 63x water objective. The fluorescence was visualized with an Argon laser at 488 nm (GFP), 514 nm (YFP) and 457 nm (CFP) with 522-532 nm (GFP), 527-560 nm (YFP) and 467-499 nm (CFP) emission filters. The images were processed by ImageJ software (http://rsb.info.nih.gov/ij/) and assembled in Adobe Photoshop CS2.

Statistical analysis

The root length was compared between 10-day-old *PIN2V* and *PIN2V SA*, or 14-day-old Col WT and *pid wag1 wag2* seedlings (n = 20). The root collapse frequency was compared between seedlings of the same age of lines *35S::PID PIN2V* (n = 180) and *35S::PID PIN2V S1,2,3A* (n = 131). To test for significant differences, we used the two-sided Student's *t*-test assuming unequal variance.

Accession numbers

The *Arabidopsis* Genome Initiative locus identifiers for the genes mentioned in this manuscript are as follows: *PID* (At2g34650), *WAG1* (At1g53700), *WAG2* (At3g14370), *AGC1-1* (At5g55910), *AGC1-2* (At4g26610), *PK5* (At5g47750), *PK7* (At3g27580), *AGC2-1* (At3g25250), *AGC2-2* (At4g31000), *AGC2-3* (At1g51170), *PIN1* (At1g73590), *PIN2* (At5g57090).

Acknowledgements

The authors thank Gerda Lamers (IBL, University of Leiden), Erik Manders and Ronald Breedijk (SILS, University of Amsterdam) for their assistance with confocal microscopy, and Ward de Winter and Werner Helvensteyn for their help with respectively tissue culture and technical assistance. This work was funded through grants from the Chinese Science Council (F.H.), from the Research Council for Earth and Life Sciences (G.C., ALW 813.06.004 to R.O.) and from the Netherlands Organisation for Health Research and Development (ZON 050-71-023 to R.O.), with financial aid from the Dutch Organization of Scientific Research (NWO), and from the Human Frontier Science Program fellowship (A.P.M.), the EMBO Young Investigator Program (to J.F.), the Odysseus Programme of the Research Foundation-Flanders (to J.F.), and by a personal fellowship from the Friedrich Ebert Stiftung (to J.K.-V.).